DOI: 10.1002/adsc.201000171

Ring Expansion *versus* Cyclization in 4-Oxoazetidine-2-carbaldehydes Catalyzed by Molecular Iodine: Experimental and Theoretical Study in Concert

Benito Alcaide,[a,*] Pedro Almendros,[b,*] Gema Cabrero,[a] Ricardo Callejo ,[a] M. Pilar Ruiz,[a] Manuel Arnó,[c] and Luis R. Domingo[c,*]

[a] Grupo de Lactamas y Heterociclos Bioactivos, Departamento de Química Orgánica I, Unidad Asociada al CSIC, Facultad de Química, Universidad Complutense de Madrid, 28040 Madrid, Spain
Fax: (+34)-91-394-4103; e-mail: alcaideb@quim.ucm.es

[b] Instituto de Química Orgánica General, Consejo Superior de Investigaciones Científicas, CSIC, Juan de la Cierva 3, 28006 Madrid, Spain
Fax: (+34)-91-564-4853; e-mail: Palmendros@iqog.csic.es

[c] Departamento de Química Orgánica, Universidad de Valencia, C/ Dr. Moliner 50, 46100 Burjassot, Valencia, Spain
Fax: (+34)-96-354-3880; e-mail: domingo@utopia.uv.es

Received: March 5, 2010; Revised: May 31, 2010; Published online: July 7, 2010

Supporting information for this article is available on the WWW under http://dx.doi.org/10.1002/adsc.201000171.

Abstract: Molecular iodine (10 mol%) efficiently catalyzes the ring expansion of 4-oxoazetidine-2-carbaldehydes in the presence of *tert*-butyldimethylsilyl cyanide, or allylic and propargylic trimethylsilanes to afford protected 5-functionalized-3,4-dihydroxypyrrolidin-2-ones with good yield and high diastereoselectivity, through a C3–C4 bond cleavage of the β-lactam nucleus. Interestingly, in contrast to the iodine-catalyzed reactions of 3-alkoxy-β-lactam aldehydes which lead to the corresponding γ-lactam derivatives (rearrangement adducts), the reactions of 3-aryloxy-β-lactam aldehydes under similar conditions gave β-lactam-fused chromanes (cyclization adducts) as the sole products, through exclusive electrophilic aromatic substitution involving the C3 aromatic ring and the carbaldehyde. In order to support the mechanistic proposals, theoretical studies have been performed.

Keywords: aldehydes; catalysis; iodine; lactams; reaction mechanisms

Introduction

β-Lactams are not only the most commonly prescribed antibacterial agents,[1] but also the use of the β-lactam nucleus as chiral building block to prepare α- and β-amino acids, alkaloids, heterocycles, taxoids, and other types of compounds of biological and medicinal interest is now well established.[2] However, although many efforts have been made in this field, there is a lack of information on the direct conversion of β-lactam aldehydes into the pharmacologically relevant pyrrolidine core. In particular, iminosugars based on polyhydroxylated pyrrolidines have attracted a great deal of attention due to the range of biological activities they show, exhibiting action as inhibitors of the enzymes α-galactosidase, α-glucosidase, and glycosidase.[3]

On the other hand, iodine-catalyzed reactions have captured much recent attention because of the low cost, ready availability, environmentally benign character, and high tolerance to air and moisture of molecular iodine.[4] In a preliminary study,[5] a single-step catalytic ring expansion approach from 4-oxoazetidine-2-carbaldehydes to enantiopure 5-cyano-3,4-dihydroxypyrrolidin-2-ones was achieved by the use of molecular iodine in the presence of *tert*-butyldimethylsilyl cyanide. The reactivity observed in the above reactions was substantially different from that reported for related simple catalysts and suggested that it was strongly modulated by the nature of the catalyst.[6] Albeit starting from slightly different substrates and triggered by different reaction conditions, the conversion of 3-alkoxy-4-(1-haloalkyl)azetidin-2-ones into 3-alkoxypyrrolidin-2-ones proceeds *via* a closely related mechanistic protocol, and may be considered

an analogue β- to γ-lactam ring expansion.[7] Following our commitment in β-lactam chemistry and catalytic processes of synthetic utility,[8] in this paper we report a systematic investigation of the iodine-catalyzed ring expansion of 4-oxoazetidine-2-carbaldehydes that fully confirms and extends our earlier conclusions and establishes a regio- and stereocontrolled versatile route to a variety of enantiopure 5-functionalized-3,4-dihydroxypyrrolidin-2-ones, together with a chemodivergent reactivity, namely, the Friedel–Crafts cyclization to β-lactam fused chromanes. Besides, the mechanisms of these iodine-catalyzed reactions have been theoretically investigated.

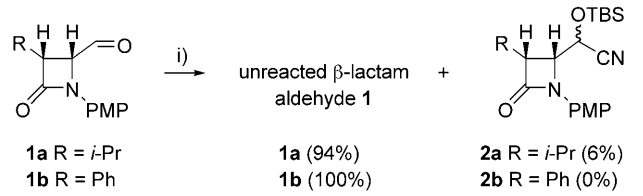

Scheme 1. Reaction of 3-alkyl(aryl)-4-oxoazetidine-2-carbaldehydes **1a** and **1b** with TBSCN under iodine catalysis. *Reagents and conditions:* i) TBSCN (3 equiv.), 10 mol% I_2, MeCN, room temperature, 6 h. TBSCN = *tert*-butyldimethylsilyl cyanide, PMP = 4-$MeOC_6H_4$.

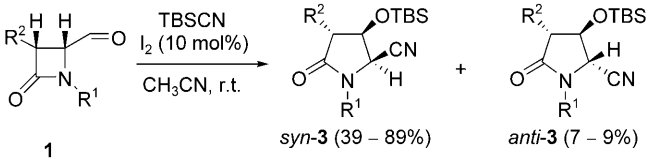

Scheme 2. Diastereoselective ring expansion of β-lactam aldehydes **1** to masked pyroglutamic acid derivatives **3** catalyzed by molecular iodine in the presence of TBSCN.

Results and Discussion

Taking into account both that iodine has been identified as a mild catalyst to promote the addition of trimethylsilyl cyanide to aldimines and ketones,[9] as well as our recent contribution on the Lewis acid-catalyzed hydrocyanation of β-lactam aldehydes,[6] we decide to test the mild Lewis acidity associated with iodine for the cyanosilylation of 4-oxoazetidine-2-carbaldehydes.

Starting substrates, 4-oxoazetidine-2-carbaldehydes **1a–r**, were prepared both in the racemic form and in optically pure form using standard methodology. Racemic compounds **1a** and **1b** were obtained as single *cis*-diastereoisomers, following our one-pot method from *N*,*N*-di-(*p*-methoxyphenyl)glyoxaldiimine.[10] Enantiopure 2-azetidinones **1c–l**, were prepared using standard methodology as single *cis*-enantiomers from imines of (*R*)-2,3-*O*-isopropylideneglyceraldehyde, through Staudinger reaction with the corresponding alkoxy(aryloxy)acetyl chloride in the presence of Et_3N, followed by sequential acidic acetonide hydrolysis and oxidative cleavage.[10] Enantiopure spiranic or 3-substituted 3-alkoxy-β-lactam aldehydes **1m** and **1n** were prepared from (*S*)-4-[(*S*)-2,2-dimethyl-1,3-dioxolan-4-yl]-1-(4-methoxyphenyl)azetidine-2,3-dione *via* metal-mediated Barbier-type carbonyl addition reactions in aqueous media followed by functionalization reactions, as we recently described.[11] Optically pure *trans*-4-oxoazetidine-2-carbaldehyde *epim*-**1c** was prepared adopting literature methodology.[12] Initial attempts to promote the cyanosilylation reaction of 4-oxoazetidine-2-carbaldehydes with *tert*-butyldimethylsilyl cyanide (TBSCN) were performed with 3-alkyl(aryl) substrates **1a** and **1b** by the use of molecular iodine as the catalyst. Unfortunately, the starting aldehyde was recovered as the main component together with small amounts of the *O*-silylated cyanohydrin **2a** when a three-fold excess of TBSCN was used (Scheme 1).

Next, we turned our attention to 3-alkoxy-4-oxoazetidine-2-carbaldehydes, and so we treated β-lactam aldehyde **1c** with TBSCN under molecular iodine catalysis. To our delight, we obtained instead of the expected β-lactam cyanohydrin the enantiopure 5-cyano-3,4-dihydroxypyrrolidin-2-one **3c** in 89% yield (Scheme 2, see also Supporting Information, Table S1), which can be regarded as a hybrid of the pharmacologically relevant subunits of iminosugar and pyroglutamic acid.[13] This result may be explained through a C3−C4 bond cleavage of the 2-azetidinone nucleus followed by rearrangement; the ring expansion reaction not being compatible with C3 substituents at the β-lactam ring different from alkoxy groups (aldehydes **1a** and **1b**, see Scheme 1). When identical conditions were applied to 4-oxoazetidine-2-carbaldehydes **1d–l**, similar rearrangement reactions occurred to afford the corresponding adducts **3d–l** in good yields (Scheme 2, see also Supporting Information, Table S1). Gratifyingly, when the reaction was not totally stereoselective, in all cases the diastereomeric adducts *syn*-**3** and *anti*-**3** could be easily separated by gravity flow chromatography, the isomeric products *anti*-**3** being the less polar compounds. The cyclic structures and the stereochemistry of masked pyroglutamic acid derivatives **3** were established by one- and two-dimensional NMR techniques and NOE experiments. The values for vicinal coupling constants (see Supporting Information, Table S2) show unequivocally an *anti/syn* orientation for protons H3–H4/H4–H5 in compounds *syn*-**3** and *anti/anti* in compounds *anti*-**3**, in agreement with that reported in the literature for related products.[14]

At this point, we became intrigued as to whether appropriately selected silylated nucleophiles different

from TBSCN, for instance, allylic and propargylic trimethylsilanes, could be used for the iodine-catalyzed ring expansion reaction. In the event, mixtures of separable isomers were in general obtained in moderate or good combined yields (56–80%). When the resulting reaction mixtures were subjected to column chromatography, 5-functionalized-2-pyrrolidinones **4** (major product, except for aldehyde **1h**), along with homoallylic alcohols (Sakurai products) **5** and morpholinones **6**, were obtained. The most significant results for different 3-alkoxy-4-oxoazetidine-2-carbaldehydes are summarized in Scheme 3.

In order to show the capacity of the method to prepare an array of γ-lactams bearing chemical diversity, several functionalities of the 2-pyrrolidinone nucleus in γ-lactam *syn*-**3c** were selectively manipulated (Scheme 4). Thus, the controlled reduction of the cyano group in the γ-lactam cyanohydrin derivative *syn*-**3c** with $NaBH_4/NiCl_2$ and subsequent Boc protection, chemospecifically afforded aminoalkylpyrrolidinone **7**.[15] Chemoselective cleavage of the TBS and PMP protecting groups under standard conditions, yielded γ-lactams **8** and **9** bearing free amino and hydroxy functionalities.

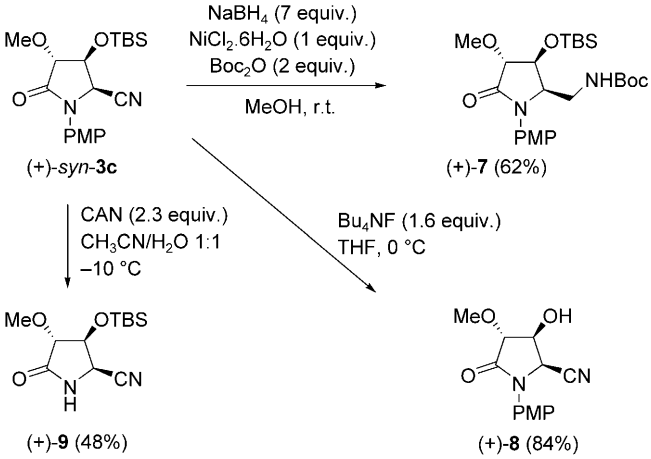

Scheme 4. Selective manipulations of polyfunctional γ-lactam *syn*-**3c**. PMP = 4-$MeOC_6H_4$, TBS = *tert*-butyldimethylsilyl.

We subsequently wished to expand the scope of our study to include aryloxy substituents at the C3 position of the β-lactam ring. Thus, several 3-aryloxy-4-oxoazetidine-2-carbaldehydes **1o–r**, were treated with molecular iodine. A smooth reaction took place, but

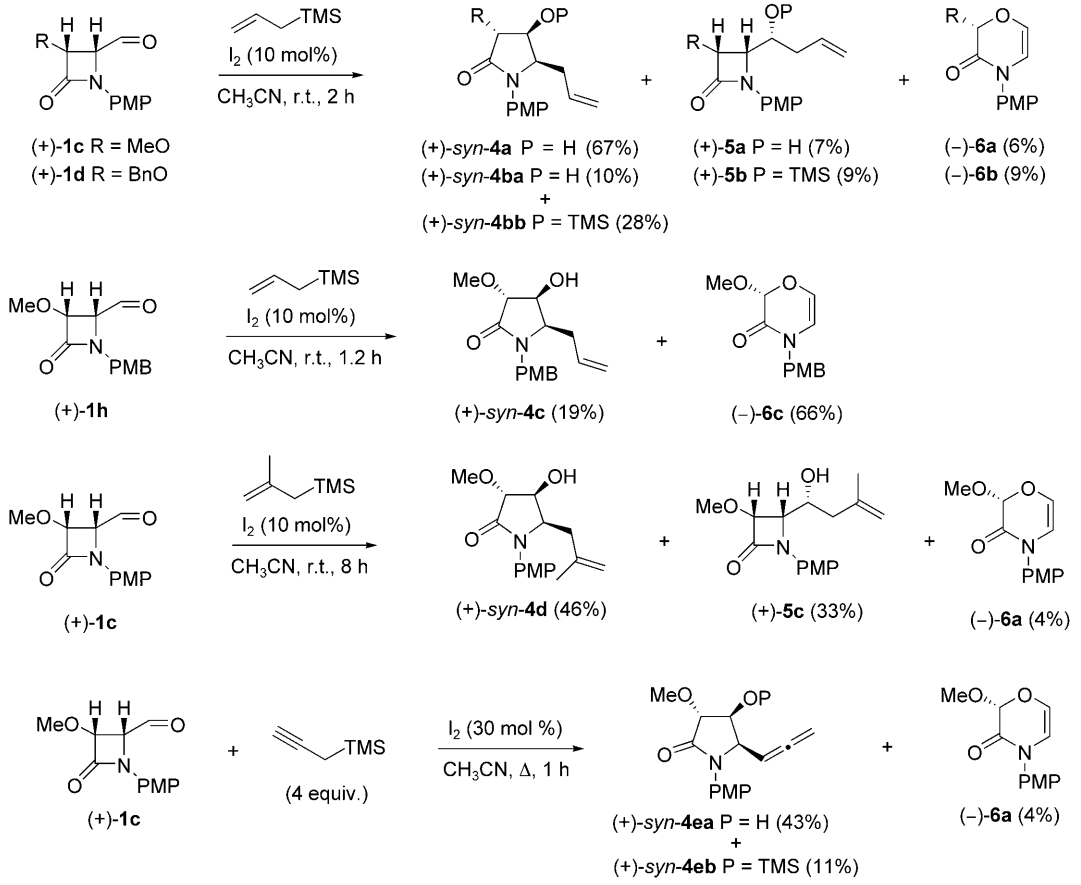

Scheme 3. Molecular iodine-catalyzed reaction in the presence of unsaturated trimethylsilanes of 4-oxoazetidine-2-carbaldehydes **1c**, **1d**, and **1h**. PMP = 4-$MeOC_6H_4$, TMS = trimethylsilyl.

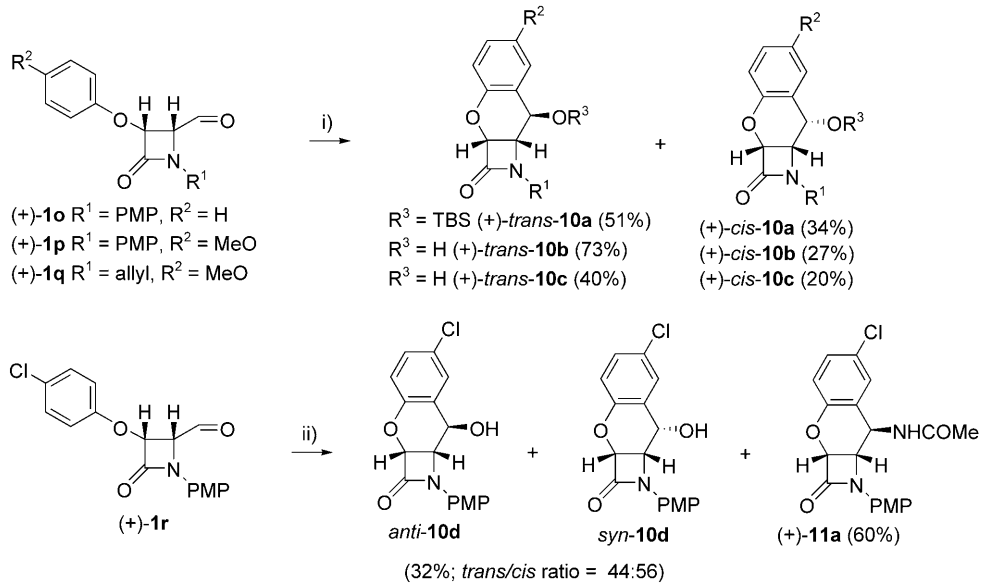

Scheme 5. Cyclization of 3-aryloxy-β-lactam aldehydes **1o–r** to β-lactam-fused chromanes **10** and **11** catalyzed by molecular iodine in the presence of TBSCN. *Reagents and conditions:* i) TBSCN (2 equiv.), 50 mol% I_2, MeCN, room temperature, **10a**: 1 h; **10b**: 72 h; **10c**: 17 h. ii) TBSCN (2 equiv.), 100 mol% I_2, MeCN, reflux, 72 h. TBSCN = *tert*-butyldimethylsilyl cyanide, PMP = 4-$MeOC_6H_4$.

the expected γ-lactams were not detected; instead the corresponding fused tricyclic β-lactams **10a–d**,[16] were isolated in fair yields (60–100%) as mixtures of separable epimers at the carbinolic-like carbon (Scheme 5). We observed that increasing the amount of iodine from 10 mol% to 50 mol% had a benefitial impact on the overall yield of the β-lactam-fused chromanes. Except for tricyclic 2-azetidinone **10a**, the TBS group was not incorporated into the final product; however, the absence of TBSCN as reaction reagent considerably diminished the conversion. The chloro-β-lactam **1r** needed forcing conditions (100 mol% of iodine, reflux) for the reaction to occur; affording amide **11a** as the major product, along with β-lactam-fused chromanes **10d** (Scheme 5). The formation of amide **11a** must be explained by invoking a Ritter reaction with the participation of the solvent (acetonitrile) and the promotion of the mild Lewis acid iodine.

Taking into account the formation of amide **11a**, we decided to explore the exposure of alcohols **10b** under usual Ritter reaction conditions.[17] Thus, the use of epimeric tricycles *trans*-**10b** and *cis*-**10b** as the alcoholic substrates in the presence of a catalytic amount of sulphuric acid as the proton source, resulted in the clean formation of amide **11b** as single isomer (Scheme 6). Later on and in view of the above results, it seemed to us interesting to analyze the behaviour of **10b** under modified Ritter conditions, running the reaction in dichloromethane and replacing acetonitrile by *tert*-butyldimethylsilyl chloride. In the event, alcohol *cis*-**10b** remained unreacted while its

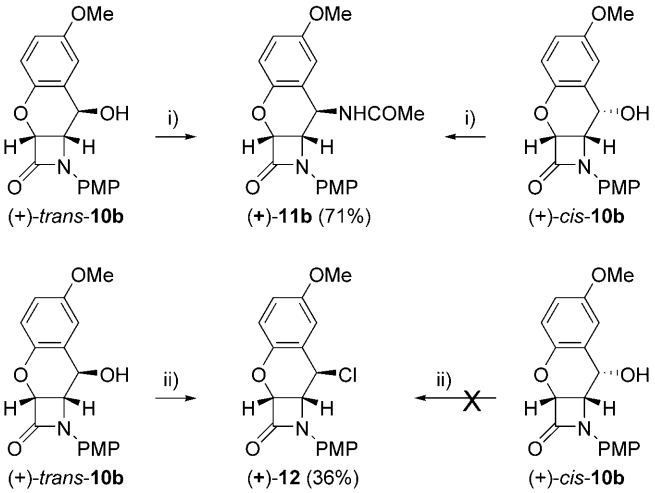

Scheme 6. Selective manipulations of β-lactam-fused chromanols *trans*-**10b** and *cis*-**10b**. *Reagents and conditions:* i) H_2SO_4 (10% vol), MeCN, room temperature, 17 h. ii) TBSCl (2 equiv.), 50 mol% I_2, CH_2Cl_2, room temperature, 22 h. PMP = 4-$MeOC_6H_4$, TBS = *tert*-butyldimethylsilyl.

epimer *trans*-**10b** was converted into the chloroadduct **12** (Scheme 6).

The tricyclic structure and the stereochemistry of β-lactam-fused chromanes **10–12** were established by one- and two-dimensional NMR techniques and NOESY-1D experiments. It should be noted that, although considerable synthetic progress has been made in the area of bicyclic β-lactam antibiotics (1,4-fused β-lactams), to date, the construction of related

3,4-fused bicyclic β-lactams containing heteroatoms like oxygen in the second heterocyclic core comprises an interesting synthetic challenge as an alternative for the conventional bicyclic 2-azetidinones.[18]

In order to understand these iodine-catalyzed reactions, the mechanism for the iodine-catalyzed ring expansion of β-lactam aldehydes was investigated using DFT methods (see Computational Methods). We selected 4-oxoazetidine-2-carbaldehyde **13** as a theoretical model, a very closely related structure to the parent precursors. Additionally, we also selected trimethylsilyl cyanide (TMSCN) to simulate the silicon reagent. The iodine-catalyzed ring expansion has a stepwise mechanism that comprises several consecutive steps (see Scheme 7). These steps can be gathered in two differentiated processes: i) the iodine-promoted ring expansion of the 4-oxoazetidine-2-carbaldehyde complex **14** to yield the zwitterionic intermediate **16**, and ii) the capture of this intermediate by TMSCN to yield complex **19**. The total and relative energies in acetonitrile are given in Table 1.

At the iodine molecule, the I7–I8 bond cleavage has a large energy, 62.4 kcal mol^{-1}. Consequently, we considered molecular iodine as the catalyst along the ring expansion process. Coordination of molecular iodine to the aldehyde oxygen atom of **13** affords complex **14**, which is 4.8 kcal mol^{-1} more stable than the separated reagents. From **14**, the C3–C4 bond cleavage affords the zwitterionic intermediate **15**, which through an electrophilic attack of the carbenium ionic C3 carbon to the carbonyl C5 carbon yields the zwitterionic intermediate **16**. The intermediate **15** is 21.5 kcal mol^{-1} higher in energy than the complex **14** as a consequence of the large zwitterionic character of this species. However, with a very low activation energy, 0.9 kcal mol^{-1}, **15** is converted *via* **TS1** in the zwitterionic intermediate **16** through the formation of the C3–C5 bond. Formation of **16** is endothermic by 11.5 kcal mol^{-1}. All attempts to locate the transition state (TS) associated with the C3–C4 bond cleavage were unsuccessful because of the large endothermic character of **15**; this fact suggesting that the corresponding TS might be energetically and geometrically closer to **15**.[19]

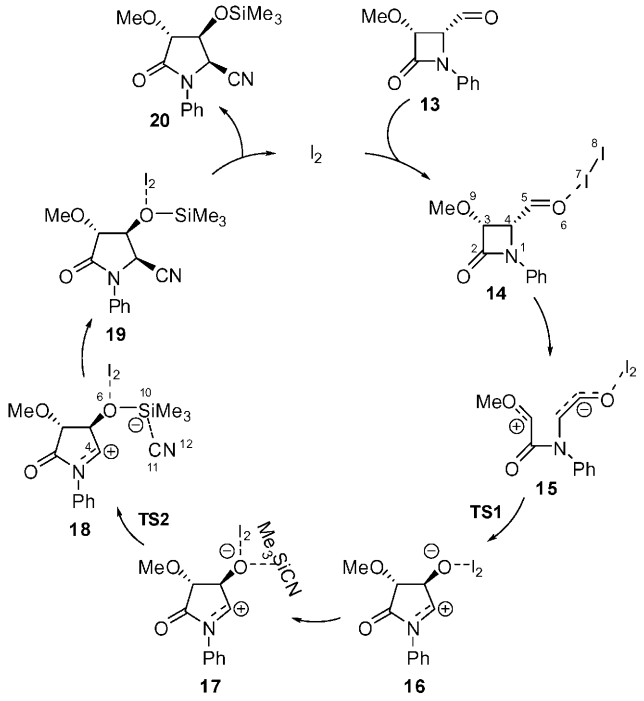

Scheme 7. Proposed catalytic cycle for the formation of pyrrolidin-2-one derivative **20** from 4-oxoazetidine-2-carbaldehyde **13**.

Table 1. Total (E, in a.u.) and relative[a] energies (ΔE, in kcal mol^{-1}) in acetonitrile of the stationary points involved in the iodine-catalyzed ring expansion of the 4-oxoazetidine-2-carbaldehyde **13**.

	B3LYP/6-31G*		B3LYP/6-31+G*	
	E	ΔE	E	ΔE
14	−14486.222221		−14486.259139	
15	−14486.187734	21.6	−14486.226205	20.7
TS1	−14486.186493	22.4	−14486.224685	21.6
16	−14486.203846	11.5	−14486.241052	11.4
17	−14988.332917		−14988.379030	
TS2	−14988.291038	26.3	−14988.339285	24.9
18	−14988.292285	25.5	−14988.341087	23.8
19	−14988.394131	−38.4	−14988.438826	−37.5

[a] Relative to **14** or **17**.

These energy results indicate that the ring expansion with formation of the zwitterionic intermediate **16** is a reversible process. However, in presence of TMSCN, intermediate **16** can be trapped to yield irreversibly the final pyrrolidin-2-one **20**. The heterolytic Si10–C11 bond cleavage at TMSCN to yield the TMS cation and the cyanide anion was also discarded because of this process is energetically very unfavourable, 79.7 kcal mol^{-1}. Due to the large negative charge located at the O6 oxygen of **16**, it is expected that this oxygen atom could produce a nucleophilic attack to the Si10 atom of TMSCN with displacement of the cyanide anion. Thus, after formation of the molecular complex **17**, the nucleophilic attack of the O6 oxygen to the Si10 atom causes the formation of the intermediate **18**, *via* **TS2. TS2** presents a large activation energy, 26.3 kcal mol^{-1}, probably due to the presence of molecular iodine in **17** that decreases the nucleophilic character of the O6 oxygen atom. Formation of **18** is also strongly endothermic, 25.5 kcal mol^{-1}. However, with an unappreciable barrier, the cyanide C11 carbon causes a nucleophilic attack to the carbenium ionic C4 atom of **18** to yield irreversibly the complex **19**. Formation of **19** from the intermediate **17** is exothermic by 38.4 kcal mol^{-1} (see Table 1).

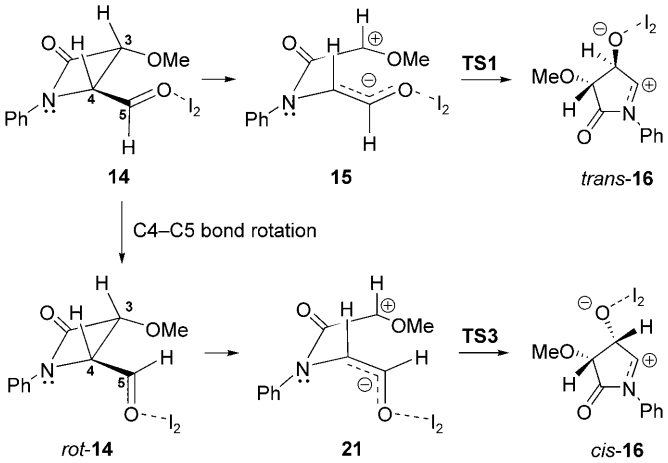

Scheme 8. Reactive channel associated with the formation of intermediates *cis*-**16** and *trans*-**16**.

These ring expansions are diastereoselective to give only the formation of *trans*-pyrrolidin-2-ones such as **20**. The MeO–OTMS *trans* relationship is obtained through a stereoselective ring closure at the intermediate **15** *via* **TS1**. In order to understand the diastereoselectivity, the reactive channel associated with the formation of the intermediate *cis*-**16** was investigated (see Scheme 8). Formation of *cis*-**16** requires the intramolecular electrophilic attack of the C3 carbenium ionic center of intermediate **21** to the C5 carbon of the C4–C5–O6 *Z*-enolate. Note that at intermediate **15**, the C4–C5–O6 enolate framework has the *E* configuration. Because of the C4–C5 bond rotation on intermediates **15** and **21** is restricted, due to the some π character of this bond, the formation of the *Z*- and *E*-enolates should take place at the ring apertures of the β-lactams **14** and *rot*-**14**, respectively. The conformer *rot*-**14** is 0.3 kcal mol^{-1} more stable than that of **14**. In consequence, through a free C4–C5 bond rotation these rotamers are in equilibrium. In addition, the zwitterionic intermediate **21** is only 1.6 kcal mol^{-1} higher in energy than **15**. Although the TS associated with the C3–C4 bond cleavage of *rot*-**14** cannot be located, it is expected that the TSs associated with the C3–C4 bond cleavage at **14** and *rot*-**14** have similar energies. However, the formation of the intermediate *cis*-**16** *via* **TS3** presents a large activation energy, 32.1 kcal mol^{-1}. That is, **TS3** is located 9.4 kcal mol^{-1} above **TS1**. This large energy difference means that, although the conformer **14** and *rot*-**14** and even the zwitterionic intermediates **15** and **21** could be in equilibrium, only the reactive channel associated with the formation of *trans*-**16** *via* **TS1** can be operative in the ring expansion process. Note that although the formation of **15** is strongly endothermic, the irreversible capture of this species by TMSCN displaces the reaction towards the formation of the *trans*-pyrrolidin-2-one **20**.

Compound *epim*-**1c** does not suffer the ring expansion in standard conditions (see Scheme 2). In order to explain this result, the ring expansion at the molecular complex *epim*-**14** was also investigated (see Scheme 9). Now, intermediate **22** is located 31.3 kcal mol^{-1} above the complex *epim*-**14**, while the activation energy associated with ring closure *via* **TS4** is 31.4 kcal mol^{-1}. These energy results indicate that both **22** and **TS4** are located *ca.* 9 kcal mol^{-1} above **15** and **TS1** (Table 2). These high energies associated with the ring expansion of the *epim*-**14** account for the experimental observation that *epim*-**1** does not undergo the ring expansion under standard reaction conditions.

The geometries of the TS and intermediates involved in the iodine-catalyzed ring expansion are depicted in Figure 1. At the zwitterionic intermediate **15** the distances between the C3 and C4 and C5 atoms are 2.455 and 2.515 Å, respectively. At **15** the distance between O6 and I7 atoms, 2.356 Å, is shorter than that at the molecular complex **14**, 2.699 Å, as a consequence of the larger interaction of the iodine mole-

Table 2. B3LYP/6-31G* Total (E, in u.a.) and relative[a] energies (ΔE, in kcal mol^{-1}) in acetonitrile of the stationary points involved in the iodine-catalyzed formation of the zwitterionic intermediates *cis*-**16** and *epim*-**16**.

	E	ΔE
rot-**14**	−14486.222640	
21	−14486.185262	23.5
TS3	−14486.171547	32.1
cis-**16**	−14486.201376	13.3
epim-**14**	−14486.222869	
22	−14486.172872	31.4
TS4	−14486.172784	31.4
epim-**16**	−14486.198585	15.2

[a] Relative to *rot*-**14** or *epim*-**14**.

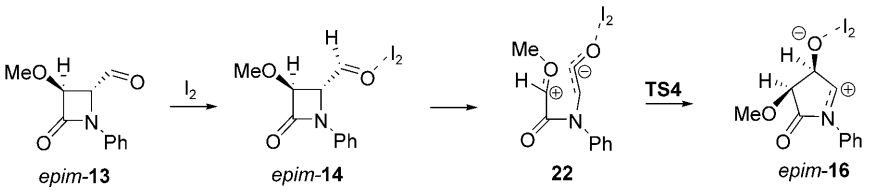

Scheme 9. Reactive channel associated with the formation of intermediate *epim*-**16**.

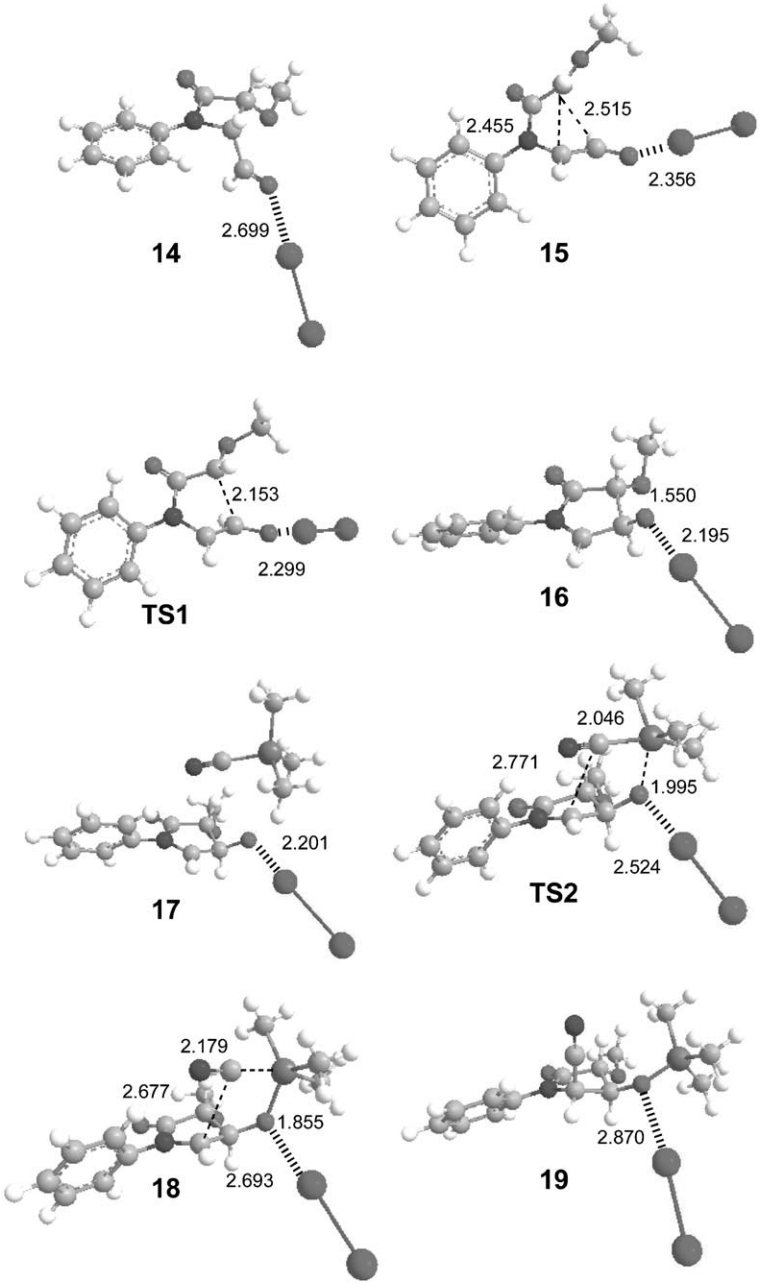

Figure 1. Geometries of the TS and intermediates involved in the iodine-catalyzed ring expansion of 4-oxoazetidine-2-carbaldehyde **13**. The distances are given in Å.

cule with the enolic O6 oxygen atom of **15** than with the carbonyl O6 oxygen atom of **14**. At **TS1** the length of the C4–C5 forming-bond is 2.153 Å. At this TS, the analysis of the atomic movement associated with the unique imaginary frequency, $-151.6\ cm^{-1}$, indicates that it is mainly associated with the C3–C5 bond formation. Analysis of the eigenvalues associated to the C3–C4 and C3–C5 bonds of the transition vector of **TS1**,[20] 0.0853 and 0.7368, indicates that at this TS the C3–C4 bond cleavage and C3–C5 bond formation are not coupled. This fact justifies the stepwise nature of the ring expansion. At the intermediate **16** the length of the C3–C5 bond is 1.550 Å; this intermediate presents the shorter O6–I7 distance, 2.195 Å.

At the complex intermediate **17**, the distance between the alkoxidic O6 oxygen atom and the Si10 atom is 3.8 Å. This intermediate opens the reactive channel associated with the nucleophilic attack of the alkoxidic O6 oxygen to the Si10 atom of TMSCN. At **TS2**, the length of the O6–Si10 forming-bond is 1.995 Å, while the length of the Si10–C11 bond, 2.046 Å, is slightly larger than that at **17**, 1.898 Å. At **TS2** the analysis of the atomic movement associated with the unique imaginary frequency, $-112.3\ cm^{-1}$, in-

dicates that it is mainly associated with the O6–Si10 bond formation. At intermediate **18**, the length of the O6–Si10 bond is 1.885 Å, whereas the length of the Si10–C11 bond remains at 2.179 Å. The distance between C4 and C11 atoms is 2.677 Å. At both **TS2** and **18** the lengths of O6–Si10 and Si10–C11 bonds indicate that the Si10 atom is pentacoordinated in these species. Finally, at molecular complex **19**, the lengths of O6–Si10 and C4–C11 bonds are 1.715 and 1.482 Å, respectively.

The geometries of **TS3** and **TS4** are depicted in Figure 2. At these TS, the lengths of the C3–C5 forming-bond, 2.015 Å (**TS3**) and 2.217 Å (**TS4**), are similar to that at **TS1**. In order to understand the higher activation energy associated with **TS3** and **TS4** than **TS1**, a conformational analysis along the C3–C5 forming-bond at the three TS was performed (see Figure 3).[21] Two geometrical parameters at these TS are analyzed: the distance between the O6 and O9 oxygen atoms and the O6–C5–C3–O9 dihedral angles. The most favourable **TS1** presents the largest O6–O9 distance, 3.605 Å. In addition, this transition state presents the largest O6–C5–C3–O9 dihedral angle, 75.2 degrees. These geometrical parameters suggest that the two O6 and O9 oxygen atoms, which could present some unfavourable electronic interactions at the corresponding TS, are further apart at the most favourable **TS1**. In addition, while **TS1** presents one C–C–C–C and one O–C–C–O *gauche* interaction, **TS3** and **TS4** present one C–C–C–C, one C–C–C–O and one O–C–C–O *gauche* interactions. Therefore, at the less favourable **TS3** and **TS4** there is an additional C–C–C–O *gauche* interaction, which is not present at **TS1** (see Figure 3).

The extent of bond cleavage or bond formation along a reaction pathway is provided by the concept of bond order (BO).[22] At **15**, the BO values between the C3 and C4 and C5 atoms are 0.22 and 0.14, respectively. These low values, which are not null, are a consequence of some charge delocation at this zwitterionic intermediate. The BO value of the C3–O9 bond, 1.21, points to a large delocalization of the O9 oxygen lone pair in the carbenium ionic C3 center formed through the heterolytic C3–C4 bond cleavage. At this intermediate the C4–C5 and C5–O6 BO values, 1.34 and 1.35, point to a C4–C5–O6 enolate structure. At **TS1**, the BO value of the C3–C5 forming-bond is 0.34. At **16**, the BO value of the C4–C5 bond is 0.94. At this intermediate, the C3–O9 BO value, 0.95, agrees with a single C–O bond. On the other hand, the N1–C4 BO value, 1.55, points to a large delocalization of the nitrogen N1 lone pair in the C4 carbenium ionic center of **16**. At this intermediate, the BO value between the alkoxidic O6 atom and the I7 iodine atom, 0.51, points to a large bonding interaction between the enolate and the iodine molecule. At **TS2**, the BO value of the O6–Si10 forming-bond is 0.31, while the Si10–C11 value is 0.57. At the intermediate **18**, the BO values of the O6–I7 and Si10–C11 bonds are 0.40 and 0.47, while the BO values between the C4 and the C11 and N12 are closer to 0.0.

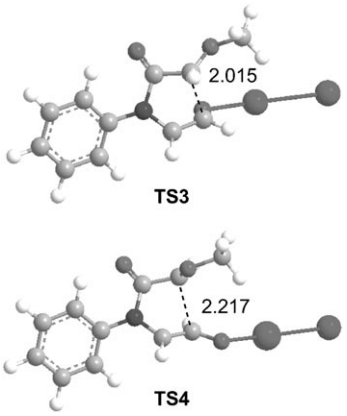

Figure 2. Geometries of **TS3** and **TS4**. The distances are given in Å.

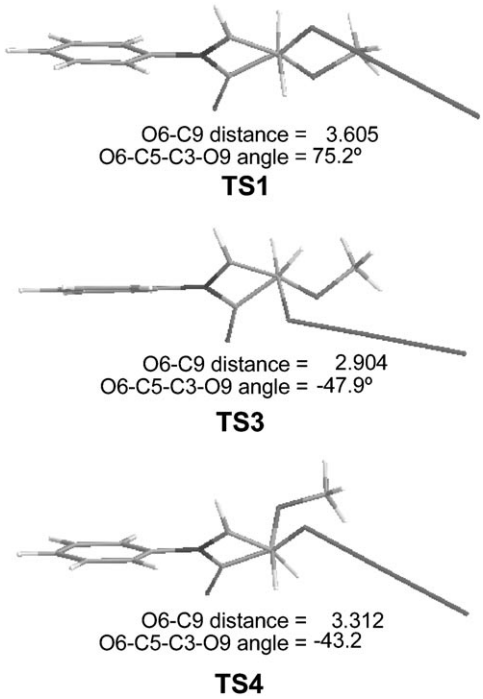

Figure 3. Stereoisomeric TS associated with C3–C5 bond formation. The O6–O9 distances are given in Å, while dihedral angles are given in degrees.

The natural charges at the I7 and I8 atoms at **14**, **15**, **TS1** and **16** are 0.04 and −0.16 e, 0.13 and −0.40 e, 0.15 and −0.47 e and 0.20 and −0.62 e, respectively. Along the ring expansion there is an increase of the charge transfer from negatively charged C4–C5–O6 enolate framework to the iodide molecule, which

presents a maximum value at **16**. The large charge transfer found at the intermediate **16**, *ca.* −0.40 e, accounts for the catalytic role of the iodine molecule to favour, together with the presence of the C3 methoxy group, the heterolytic C3–C4 bond cleavage that takes place at these ring expansion reactions. Interestingly, the non-coordinated I8 atom supports the negative charge that is being transferred at the iodine molecule catalyst.

From this DFT study we can draw some interesting conclusions about these iodine-catalyzed ring expansion reactions. i) The ring expansion process proceeds by a stepwise mechanism that involves the C3–C4 bond cleavage and the subsequent C3–C5 bond formation. In order to favour the heterolytic C3–C4 bond cleavage, the presence of an electron-releasing methoxy group at the C3 carbon, and the electron-withdrawing iodine molecule acting as a Lewis catalyst are demanded. Note that these ring expansions do not take place in the absence of the methoxy group at the C3 position. ii) The capture of the zwitterionic intermediate **16** by TMSCN takes place also through a two-step nucleophilic substitution at the Si atom with formation of a pentacoordinated Si intermediate. The subsequent transfer of the CN group from the Si atom to the carbocationic C4 center takes place *via* a concerted process. This behaviour means that the C3–C5 bond formation takes place by the same face of the pyrrolidin-2-one **17** where the $OSiMe_3$ group is located. This behaviour allows us to explain the *cis* arrangement of the $OSiMe_3$ and CN substituents at the final pyrrolidin-2-ones. iii) The higher energy associated with the C3–C5 bond formation at the conformer *rot*-**14**, allowing the formation of the *cis*-**16**, accounts for the diastereoselectivity of these ring expansion processes. Finally, iv) the high energy associated with the C3–C5 bond formation at the *epim*-**13** accounts for the observation that *epim*-**1c** does not suffer the ring expansion in standard conditions.

The differences encountered for the iodine-catalyzed ring expansion reaction between different silylated nucleophiles such as TBSCN and allyltrimethylsilane, could be explained through the different polarizability of the C–Si bond in both reagents. TBSCN bears a more polarized C–Si bond than the allylic silane, which implies that allyltrimethylsilane requires a higher activation energy for the S_N2 reaction (from **17** to **18** in Scheme 7). The formation of morpholin-3-ones **6** should proceed by a reaction course that also involves C3–C4 β-lactam bond breakage in the transition state (Scheme 10). Probably, iodine enhances the reactivity of the 2-azetidinone moiety through selective complexation to the aldehyde site. The cleavage of the C3–C4 bond is facilitated both by the enhancement of the electrophilicity of the carbonyl group as well as by the stabilization of the resulting carbocation in C3 due to the α oxygen atom. The formation of the six-membered intermediate **23** presents large activation energy, 6.0 kcal mol^{-1}, in comparison with its five-membered counterpart (intermediate **16**). However, while the formation of intermediate **16** is highly endothermic, 11.2 kcal mol^{-1}, the formation of intermediate **23** is slightly exothermic, −1.1 kcal mol^{-1}. Thus, pyrrolidin-2-one derivatives **3** come from a kinetic control and morpholin-3-ones **6** should arise from a thermodynamic control. For the TBSCN case, intermediate **16** is attacked for the sylilated reagent, irreversibly affording the final product **3**. Because the addition of allyltrimethylsilane requires more energy, the competitive mechanism for the obtention of compounds **6** *via* intermediate **23** is also operative.

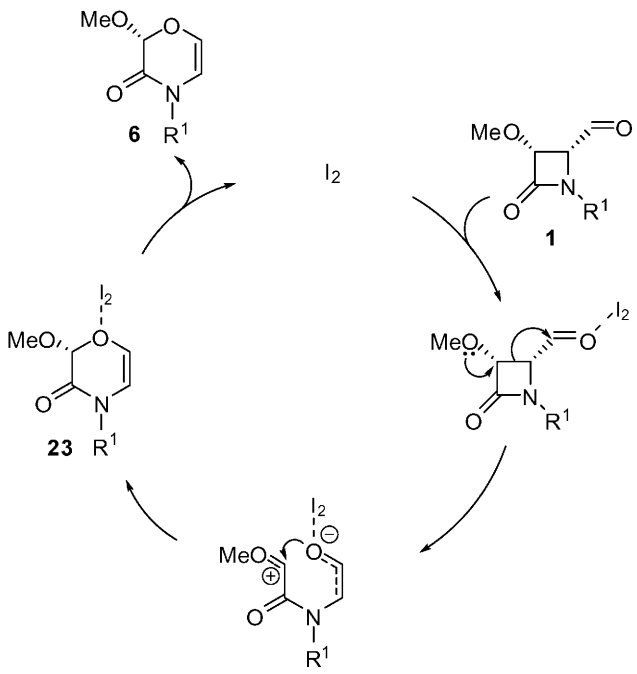

Scheme 10. Mechanistic explanation for the formation of morpholin-3-one derivatives **6**.

When the C3 substituent in the β-lactam ring is aryloxy rather than alkoxy, the disponibility of the oxygen lone pair is lower because of the delocalization at the aromatic ring. This fact may well explain the alternative way (electrophilic aromatic substitution) for the reaction to happen. A possible mechanism for the iodine-catalyzed Friedel–Crafts type cyclization may initially involve the formation of a complex **24** through coordination of elemental iodine to the aldehyde group of 3-aryloxy-4-oxoazetidine-2-carbaldehydes **1o–r**. This increase of the carbonyl group reactivity should promote an electrophilic aromatic substitution with the C3 aromatic ring, forming the six-membered Wheland-type intermediate **25**, which is stabilized by the electron pair of the α heteroatom. Subsequent deprotonation would form tricycles **26**. Finally, iodine-silicon exchange liberates adducts **10**

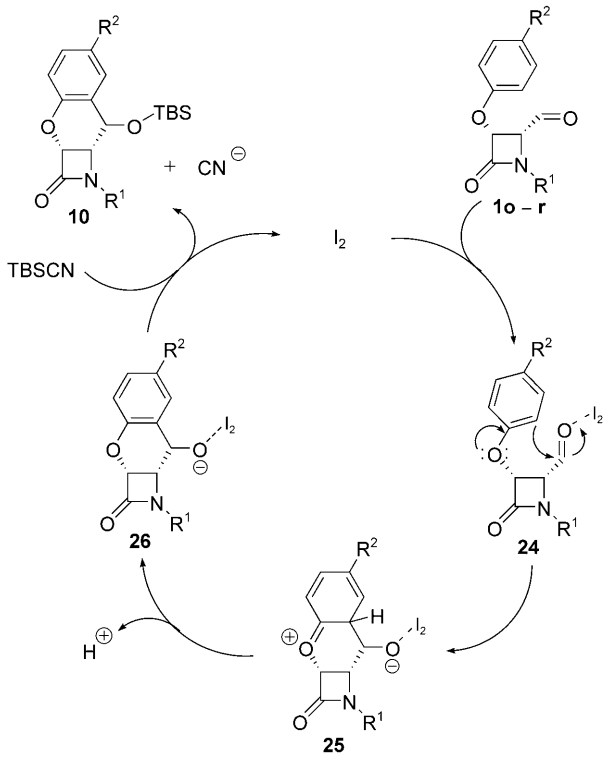

Scheme 11. Mechanistic explanation for the formation of β-lactam fused chromanes **10** under iodine catalysis.

with concomitant regeneration of the catalyst (Scheme 11).

A rational accounting for the stereochemical outcome of the cyclization reactions of β-lactam aldehydes catalyzed by iodine is depicted in Scheme 12. Thus, a six-membered cyclic chair-like transition-state model with minimization of interactions would account for the formation of tricyclic adducts *trans*-**10**.

Conclusions

In conclusion, this is the first single-step catalytic approach to the pyroglutamic acid core *via* molecular iodine-catalyzed ring expansion reaction of the β-lactam nucleus. The novel C3–C4 bond breakage of the β-lactam skeleton relies upon appropriate substitution and stereochemistry at C3. This mild protocol uses a cheap and environmentally friendly catalyst, and can install polysubstitution at the pyrrolidin-2-one ring. On the other hand, starting from 3-aryloxy-4-oxoazetidine-2-carbaldehydes a divergent reactivity, namely, the Friedel–Crafts type cyclization to β-lactam-fused chromanes was encountered. In addition, density functional theory (DFT) calculations were performed to obtain an insight into various aspects of the reactivity of 4-oxoazetidine-2-carbaldehydes under iodine catalysis.

Experimental Section

General methods

^{1}H NMR and ^{13}C NMR spectra were recorded on a Bruker AMX-500, Bruker Avance-300, Varian VRX-300S or Bruker AC-200. NMR spectra were recorded in $CDCl_3$ solutions, except where otherwise stated. Chemical shifts are given in ppm relative to TMS (^{1}H, 0.0 ppm), or $CDCl_3$ (^{13}C, 77.0 ppm). Low- and high-resolution mass spectra were taken on an Agilent 6520 Accurate-Mass QTOF LC/MS spectrometer using the electronic impact (EI) or electrospray modes (ES) unless otherwise stated. IR spectra were recorded on a Bruker Tensor 27 spectrometer. Specific rotation $[\alpha]_D$ is given in 10^{-1} deg cm^2 g^{-1} at 20 °C, and the concentration (*c*) is expressed in g per 100 mL. All commercially available compounds were used without further purification.

General Procedure for the Iodine-Catalyzed β-Lactam Ring Expansion Reaction. Preparation of 3,4-Dihydroxypyrrolidin-2-one Derivatives 3 and 4

A solution of the appropriate sylilated nucleophile (1.50–5.00 mmol) in anhydrous acetonitrile (3.4 mL) was added dropwise *via* syringe to a stirred solution of the appropriate 4-oxoazetidine-2-carbaldehyde **1** (1.00 mmol) and iodine (0.10 mmol) in the same solvent (3.4 mL) at room temperature and under an argon atmosphere. The reaction mixture was stirred at room temperature until disappearance of starting material (TLC). Then, brine (10 mL) was added and the resulting mixture was extracted with dichloromethane (DCM) (5 × 20 mL). The organic layer was dried ($MgSO_4$), filtered and concentrated under reduced pressure. Analyti-

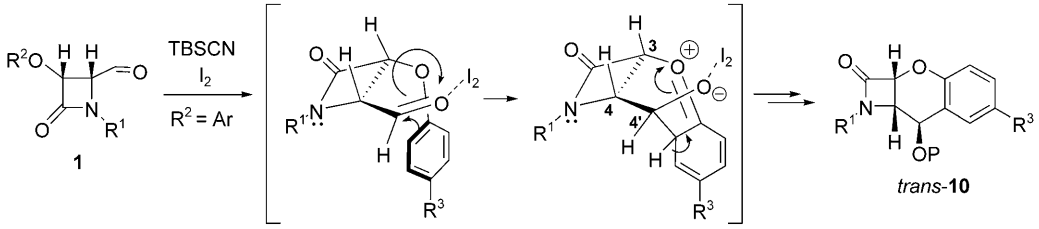

Scheme 12. Proposed model for iodine-catalyzed cyclization reaction of 4-oxoazetidine-2-carbaldehydes leading to β-lactam fused chromanes.

cally pure adducts **3** or **4** were obtained after flash chromatography of the residue on silica gel eluting with hexanes/ethyl acetate mixtures.[23]

(2*R*,3*S*,4*R*)-3-(*tert*-Butyldimethylsilyloxy)-4-methoxy-1-(4-methoxyphenyl)-5-oxopyrrolidine-2-carbonitrile [(+)-*syn*-3c]: From 1.0 g (4.26 mmol) of 4-oxoazetidine-2-carbaldehyde (+)-**1c**, and after chromatography of the residue using hexanes/ethyl acetate (5:1) as eluent gave compound (+)-*syn*-**3c** as a colourless oil; yield: 1.42 g (89%); $[\alpha]_D$: +44.9 (*c* 0.7 in $CHCl_3$); ^{1}H NMR (300 MHz, $CDCl_3$, 25 °C): δ = 7.43 (AA′**XX′**, 2H), 6.94 (**AA′**XX′, 2H), 4.68 (d, *J* = 7.3 Hz, 1H), 4.47 (t, *J* = 7.6 Hz, 1H), 4.11 (d, *J* = 7.9 Hz, 1H), 3.81 (s, 3H), 3.75 (s, 3H), 0.97 (s, 9H), 0.20 (s, 3H), 0.19 (s, 3H); ^{13}C NMR (75 MHz, $CDCl_3$, 25 °C): δ = 169.3, 158.4, 129.3, 124.1, 115.1, 114.6, 82.6, 71.9, 59.7, 55.5, 53.8, 25.5, 17.9, −4.8, −5.1; IR ($CHCl_3$): ν = 1727 cm^{-1}; MS (EI): *m/z* (%) = 376 (15) $[M]^+$, 319 (100) $[M-57]^+$; elemental analysis calcd. (%) for $C_{19}H_{28}N_2O_4Si$ (376.5): C 60.61, H 7.50, N 7.44; found: C 60.51, H 7.42, N 7.54.

(3*R*,4*S*,5*R*)-5-Allyl-4-hydroxy-3-methoxy-1-(4-methoxyphenyl)pyrrolidin-2-one [(+)-*syn*-4a]: From 50 mg (0.21 mmol) of 4-oxoazetidine-2-carbaldehyde (+)-**1c**, and after chromatography of the residue using hexanes/ethyl acetate (5:1) as eluent, 40 mg (67%) of the less polar compound (+)-*syn*-**4a**, 4 mg (7%) of compound (+)-**5a**, and 3 mg (6%) of the more polar compound (−)-**6a** were obtained.

(3*R*,4*S*,5*R*)-5-Allyl-4-hydroxy-3-methoxy-1-(4-methoxyphenyl)pyrrolidin-2-one [(+)-*syn*-4a]: Colourless solid; mp 123–125 °C; $[\alpha]_D$: +57.7 (*c* 0.5 in $CHCl_3$); ^{1}H NMR (300 MHz, $CDCl_3$, 25 °C): δ = 7.30 (AA′**XX′**, 2H), 6.92 (**AA′**XX′, 2H), 5.82 (m, 1H), 5.15–5.06 (m, 2H), 4.52 (t, *J* = 7.1 Hz, 1H), 4.26 (dt, *J* = 7.3, 5.4 Hz, 1H), 4.08 (d, *J* = 6.8 Hz, 1H), 3.81 (s, 3H), 3.72 (s, 3H), 2.45 (t, *J* = 6.1 Hz, 2H); ^{13}C NMR (75 MHz, $CDCl_3$, 25 °C): δ = 167.0, 157.8, 133.7, 129.8, 125.4, 118.9, 114.4, 83.4, 72.4, 60.4, 59.0, 55.4, 32.2; IR (KBr): ν = 3373, 1678 cm^{-1}; MS (EI): *m/z* (%) = 277 (63) $[M]^+$, 134 (100).

(3*R*,4*S*)-4-[(*R*)-1-Hydroxybut-3-enyl]-3-methoxy-1-(4-methoxyphenyl)azetidin-2-one [(+)-5a]: Pale yellow oil; $[\alpha]_D$: +127.5 (*c* 1.7 in $CHCl_3$); ^{1}H NMR (300 MHz, $CDCl_3$, 25 °C): δ = 7.41 (AA′**XX′**, 2H), 6.87 (**AA′**XX′, 2H), 5.85 (ddt, *J* = 15.9, 11.4, 6.9 Hz, 1H), 5.16–5.07 (m, 2H), 4.64 (d, *J* = 5.4 Hz, 1H), 4.31 (t, *J* = 4.8 Hz, 1H), 4.10 (m, 1H), 3.80 (s, 3H), 3.69 (s, 3H), 2.56 (d, *J* = 3.9 Hz, 1H), 2.33 (t, *J* = 6.6 Hz, 2H); ^{13}C NMR (75 MHz, $CDCl_3$, 25 °C): δ = 165.1, 156.8, 134.3, 130.7, 120.5, 117.9, 114.2, 82.7, 70.4, 60.1, 59.7, 55.5, 38.3; IR ($CHCl_3$): ν = 3468, 1743 cm^{-1}; MS (EI): *m/z* (%) = 277 (100) $[M]^+$.

(*R*)-2-Methoxy-4-(4-methoxyphenyl)-2*H*-1,4-oxazin-3(4*H*)-one [(−)-6a]: Pale orange oil; $[\alpha]_D$: −166.5 (*c* 0.5 in $CHCl_3$); ^{1}H NMR (300 MHz, $CDCl_3$, 25 °C): δ = 7.26 (AA′**XX′**, 2H), 6.94 (**AA′**XX′, 2H), 6.20 (d, *J* = 4.3 Hz, 1H), 5.94 (d, *J* = 4.4 Hz, 1H), 5.27 (s, 1H), 3.83 (s, 3H), 3.60 (s, 3H); ^{13}C NMR (75 MHz, $CDCl_3$, 25 °C): δ = 158.8, 158.6, 131.5, 126.7, 126.5, 114.5, 112.3, 97.9, 56.5, 55.5; IR ($CHCl_3$): ν = 1696 cm^{-1}; MS (EI): *m/z* (%) = 235 (37) $[M]^+$, 134 (100).

General Procedure for the Iodine-Catalyzed Cyclization of 3-Aryloxy β-lactam aldehydes. Preparation of β-Lactam-Fused Chromanes 10 and 11

A solution of *tert*-butyldimethylsilyl cyanide (1.50–5.00 mmol) in anhydrous acetonitrile (3.4 mL) was added dropwise *via* syringe to a stirred solution of the appropriate 3-aryloxy-β-lactam aldehyde **1o–r** (1.00 mmol) and iodine (0.10 mmol) in the same solvent (3.4 mL) at room temperature and under an argon atmosphere. The reaction mixture was stirred at room temperature until disappearance of starting material (TLC). Then, brine (10 mL) was added and the resulting mixture was extracted with DCM (5 × 20 mL). The organic layer was dried ($MgSO_4$), filtered and concentrated under reduced pressure. Analytically pure adducts **10** or **11** were obtained after flash chromatography of the residue on silica gel eluting with hexanes/ethyl acetate mixtures.

β-Lactam-fused chromanes (2a*R*,8*R*,8a*S*)-8-hydroxy-6-methoxy-1-(4-methoxyphenyl)-8,8a-dihydro-1*H*-chromeno[3,2-*b*]azet-2(2a*H*)-one [(+)-*trans*-10b] and (2a*R*,8*S*,8a*S*)-8-hydroxy-6-methoxy-1-(4-methoxyphenyl)-8,8a-dihydro-1*H*-chromeno[3,2-*b*]azet-2(2a*H*)-one [(+)-*cis*-10b]: From 105 mg (0.084 mmol) of 3-aryloxy-β-lactam aldehyde (+)-**1p**, and after chromatography of the residue using hexanes/ethyl acetate (3:1) as eluent, 77 mg (73%) of the less polar compound (+)-*trans*-**10b** and 28 mg (27%) of the more polar compound (+)-*cis*-**10b** were obtained.

(2a*R*,8*R*,8a*S*)-8-Hydroxy-6-methoxy-1-(4-methoxyphenyl)-8,8a-dihydro-1*H*-chromeno[3,2-*b*]azet-2(2a*H*)-one [(+)-*trans*-10b]: Colourless solid; mp 132–133 °C; $[\alpha]_D$: +161.6 (*c* 0.5 in $CHCl_3$); ^{1}H NMR (300 MHz, $CDCl_3$, 25 °C): δ = 7.34 (AA′**XX′**, 2H), 7.04 (d, *J* = 8.9 Hz, 1H), 6.87 (**AA′**XX′, 2H), 6.88–6.84 (m, 1H), 6.70 (d, *J* = 3.0 Hz, 1H), 5.40 (d, *J* = 5.1 Hz, 1H), 5.07 (d, *J* = 2.0 Hz, 1H), 4.71 (dd, *J* = 5.1, 2.1 Hz, 1H), 3.79 (s, 3H), 3.73 (s, 3H); ^{13}C NMR (75 MHz, $CDCl_3$, 25 °C): δ = 162.2, 156.7, 155.6, 146.0, 129.8, 125.2, 119.9, 118.5, 116.4, 115.2, 114.6, 79.0, 66.2, 59.2, 55.6, 55.5; IR (KBr): ν = 3413, 1747 cm^{-1}; HR-MS (ES): *m/z* = 328.1179, calcd. for $C_{18}H_{18}NO_5$ $[M+H]^+$: 328.1185.

(2a*R*,8*S*,8a*S*)-8-Hydroxy-6-methoxy-1-(4-methoxyphenyl)-8,8a-dihydro-1*H*-chromeno[3,2-*b*]azet-2(2a*H*)-one [(+)-*cis*-10b]: Colourless oil; $[\alpha]_D$: +147.7 (*c* 0.4 in $CHCl_3$); ^{1}H NMR (300 MHz, $CDCl_3$, 25 °C): δ = 7.52 (AA′**XX′**, 2H), 7.04 (d, *J* = 8.8 Hz, 1H), 7.00 (d, *J* = 2.8 Hz, 1H), 6.84 (**AA′**XX′, 2H), 6.85–6.80 (m, 1H), 5.35 (d, *J* = 5.4 Hz, 1H), 5.13 (br s, 1H), 5.00 (dd, *J* = 5.4, 4.1 Hz, 1H), 3.78 (s, 3H), 3.76 (s, 3H), 2.22 (d, *J* = 9.1 Hz, 1H); ^{13}C NMR (75 MHz, $CDCl_3$, 25 °C): δ = 163.2, 156.8, 156.0, 145.2, 130.9, 127.4, 119.5, 118.9, 114.5, 114.2, 110.4, 79.2, 68.7, 61.0, 55.6, 55.5; IR ($CHCl_3$): ν = 3430, 1740 cm^{-1}; HR-MS (ES): *m/z* = 328.1171, calcd. for $C_{18}H_{18}NO_5$ $[M+H]^+$: 328.1185.

Computational Methods

DFT calculations have been carried out using the B3LYP[24] exchange-correlation functional, together with the standard 6–31G* basis set.[25] For the iodine atoms, the standard 3–21G basis set was used. Since TSs and intermediates have a large zwitterionic character and polar solvents can modify both gas phase energies and geometries, the effects of acetonitrile was considered at the geometrical optimizations by using the polarizable continuum model (PCM) of Tomasi's group.[26] Single point energy calculation at the 6–31+G*

level using the 6–31G* geometries were performed. Minor changes were observed because of the zwitterionic species are already stabilized by the solvent effects. The optimizations were carried out using the Berny analytical gradient optimization method.[27] The stationary points were characterized by frequency calculations. The intrinsic reaction coordinate (IRC)[28] paths were traced by using the second order González–Schlegel integration method.[29] The electronic structures of stationary points were analyzed by the natural bond orbital (NBO) method.[30] All calculations were carried out with the Gaussian 03 suite of programs.[31]

Acknowledgements

Support for this work by the DGI-MICINN (Projects CTQ2006-10292, CTQ2009-09318 and CTQ2009-11027), Comunidad Autónoma de Madrid (Project S2009/PPQ-1752) and UCM-BSCH (Project GR58/08) are gratefully acknowledged. G. C. and R. C. thank the MEC for predoctoral grants.

References

[1] See, for example: a) J. Spencer, T. Walsh, *Angew. Chem.* **2006**, *118*, 1038; *Angew. Chem. Int. Ed.* **2006**, *45*, 1022; b) J. F. Fisher, S. O. Meroueh, S. Mobashery, *Chem. Rev.* **2005**, *105*, 395; c) D. Niccolai, L. Tarsi, R. J. Thomas, *Chem. Commun.* **1997**, 2333; d) R. Southgate, *Contemp. Org. Synth.* **1994**, *1*, 417; e) R. Southgate, C. Branch, S. Coulton, E. Hunt, in: *Recent Progress in the Chemical Synthesis of Antibiotics and Related Microbial Products*, (Ed.: G. Lukacs), Springer, Berlin, **1993**, Vol. 2, p 621; f) *The Chemistry of* β-*Lactams*, (Ed.: M. I. Page), Chapman and Hall: London, **1992**; g) *Chemistry and Biology of* β-*Lactam Antibiotics*, (Eds.: R. B. Morin, M. Gorman), Academic, New York, **1982**, Vols. 1–3.

[2] For selected reviews on 2-azetidinones acting as an important class of organic intermediates in organic synthesis, see: a) B. Alcaide, P. Almendros, C. Aragoncillo, *Chem. Rev.* **2007**, *107*, 4437; b) B. Alcaide, P. Almendros, *Curr. Med. Chem.* **2004**, *11*, 1921; c) A. R. A. S. Deshmukh, B. M. Bhawal, D. Krishnaswamy, V. V. Govande, B. A. Shinkre, A. Jayanthi, *Curr. Med. Chem.* **2004**, *11*, 1889; d) B. Alcaide, P. Almendros, *Synlett* **2002**, 381; e) C. Palomo, J. M. Aizpurua, I. Ganboa, M. Oiarbide, *Synlett* **2001**, 1813; f) B. Alcaide, P. Almendros, *Chem. Soc. Rev.* **2001**, *30*, 226; g) B. Alcaide, P. Almendros, *Org. Prep. Proced. Int.* **2001**, *33*, 315; h) I. Ojima, F. Delaloge, *Chem. Soc. Rev.* **1997**, *26*, 377; i) M. S. Manhas, D. R. Wagle, J. Chiang, A. K. Bose, *Heterocycles* **1988**, *27*, 1755.

[3] a) P. Compain, O. R. Martin, *Iminosugars: From Synthesis to Therapeutic Applications*, Wiley, Chichester, **2007**; b) K. L. Curtis, E. L. Evinson, S. Handa, K. Singh, *Org. Biomol. Chem.* **2007**, *5*, 3544; c) N. Asano, *Glycobiology* **2003**, *13*, 93R-104R; d) Y. Nishimura, *Curr. Top. Med. Chem.* **2003**, *3*, 575; e) N. Asano, R. J. Nash, R. J. Molyneux, G. W. J. Fleet, *Tetrahedron: Asymmetry* **2000**, *11*, 1645; f) G. Legler, in: *Iminosugars as Glycosidase Inhibitors: Nojirimycin and Beyond*, (Ed.: A. E. Stütz), Wiley-VCH, Weinheim, **1999**.

[4] For recent reviews, see: a) S. Das, R. Borah, R. R. Devi, A. J. Thakur, *Synlett* **2008**, 2741; b) H. Togo, S. Iida, *Synlett* **2006**, 2159.

[5] a) B. Alcaide, P. Almendros, G. Cabrero, M. P. Ruiz, *Chem. Commun.* **2008**, 615; b) B. Alcaide, P. Almendros, G. Cabrero, M. P. Ruiz, *Synthesis* **2008**, 2835.

[6] We have recently described the hydrocyanation and cyanosilylation of 4-oxoazetidine-2-carbaldehydes together with the manipulation of the corresponding β-lactam cyanohydrins: B. Alcaide, P. Almendros, G. Cabrero, M. P. Ruiz, *J. Org. Chem.* **2007**, *72*, 7980.

[7] a) W. Van Brabandt, N. De Kimpe, *J. Org. Chem.* **2005**, *70*, 3369; b) W. Van Brabandt, N. De Kimpe, *J. Org. Chem.* **2005**, *70*, 8717; c) S. Dekeukeleire, M. D'hooghe, N. De Kimpe, *J. Org. Chem.* **2009**, *74*, 1644.

[8] See, for instance: a) B. Alcaide, P. Almendros, R. Carrascosa, M. R. Torres, *Adv. Synth. Catal.* **2010**, *352*, 1277; b) B. Alcaide, P. Almendros, A. Luna, M. R. Torres, *Adv. Synth. Catal.* **2010**, *352*, 621; c) B. Alcaide, P. Almendros, T. Martínez del Campo, M. T. Quirós, *Chem. Eur. J.* **2009**, *15*, 3344; d) B. Alcaide, P. Almendros, R. Carrascosa, T. Martínez del Campo, *Chem. Eur. J.* **2009**, *15*, 2496; e) B. Alcaide, P. Almendros, R. Carrascosa, M. C. Redondo, *Chem. Eur. J.* **2008**, *14*, 637; f) B. Alcaide, P. Almendros, T. Martínez del Campo, *Angew. Chem.* **2007**, *119*, 6804; *Angew. Chem. Int. Ed.* **2007**, *46*, 6684.

[9] a) B. Das, P. Balasubramanyam, M. Krishnaiah, B. Veeranjaneyulu, G. C. Reddy, *Synthesis* **2009**, 3467; b) J. S. Yadav, B. V. S. Reddy, M. S. Reddy, A. R. Prasad, *Tetrahedron Lett.* **2002**, *43*, 9703.

[10] B. Alcaide, P. Almendros, *Chem. Soc. Rev.* **2001**, *30*, 226.

[11] B. Alcaide, P. Almendros, M. C. Redondo, *Eur. J. Org. Chem.* **2007**, 3707.

[12] D. R. Wagle, C. Garai, J. Chiang, M. G. Monteleone, B. E. Kurys, T. W. Strohmeyer, V. R. Hedge, M. S. Manhas, A. K. Bose, *J. Org. Chem.* **1988**, *53*, 4227.

[13] The pyroglutamic acid core has considerable chemical and medicinal importance as it is involved in a wide range of relevant processes. For reviews, see: a) S. K. Panday, J. Prasad, D. K. Dikshit, *Tetrahedron: Asymmetry* **2009**, *20*, 1581; b) C. Nájera, M. Yus, M. *Tetrahedron: Asymmetry* **1999**, *10*, 2245.

[14] M. Oba, S. Koguchi, K. Nishiyama, *Tetrahedron* **2002**, *58*, 9359.

[15] Recently, it has been demonstrated that a *cis*-5-alkyl-4-hydroxy-2-pyrrolidinone related to **7**, named as streptopyrrolidine and isolated from a marine *Streptomyces*, blocked the capillary tube formation of the cells at the same potency as a known angiogenesis inhibitor SU11248: H.-J. Shin, T.-S. Kim, H.-S. Lee, J.-Y. Park, I.-K. Choi, H.-J. Kwon, *Phytochemistry* **2008**, *69*, 2363.

[16] Tricyclic β-lactam antibiotics which are generally referred to as trinems are a new class of synthetic antibacterial agents featuring good resistance to β-lactamases and dehydropeptidases: a) O. Kanno, I. Kawamoto, *Tetrahedron* **2000**, *56*, 5639; b) S. Hanessian, B. Reddy, *Tetrahedron* **1999**, *55*, 3427; c) C. Ghiron, T. Rossi, *The Chemistry of Trinems*, in: *Targets in Hetero-*

cyclic Systems – Chemistry and Properties, (Eds.: O. A. Attanasi, D. Spinelli), Societa Chimica Italiana, Rome, **1997**, Vol. 1, pp 161–186. For a review on tricyclic β-lactams, see: d) B. Alcaide, P. Almendros, *Curr. Org. Chem.* **2002**, *6*, 245.

[17] R. Bishop, in: *Comprehensive Organic Synthesis*, (Eds.: B. M. Trost, I. Fleming), Pergamon Press, New York, **1991**, Vol. 6, pp 261–300.

[18] Little information regarding this type of oxygen-containing 3,4-fused β-lactam systems can be found in the literature. For selected examples, see: a) E. Leemans, M. D'hooghe, Y. Dejaegher, K. W. Törnroos, N. De Kimpe, *Eur. J. Org. Chem.* **2010**, 352; b) Z. Zhang, Q. Zhang, Z. Ni, Q. Liu, *Chem. Commun.* **2010**, *46*, 1269; c) B. Alcaide, P. Almendros, T. Martínez del Campo, E. Soriano, J. L. Marco-Contelles, *Chem. Eur. J.* **2009**, *15*, 1901; d) A. Al-Harrasi, F. Pfrengle, V. Prisyazhnyuk, S. Yekta, P. Kooš, H.-U. Reissig, *Chem. Eur. J.* **2009**, *15*, 11632; e) P. Del Buttero, G. Molteni, A. Papagni, T. Pilati, *Tetrahedron: Asymmetry* **2005**, *16*, 971.

[19] G. S. Hammond, *J. Am. Chem. Soc.* **1955**, *77*, 334.

[20] a) J. W. McIver, *Acc. Chem. Res.* **1974**, *7*, 72; b) L. R. Domingo, J. Andres, V. Moliner, V. S. Safont, *J. Am. Chem. Soc.* **1997**, *119*, 6415.

[21] M. Arnó, R. J. Zaragoza, L. R. Domingo, *Tetrahedron: Asymmetry* **2007**, *18*, 157.

[22] K. B. Wiberg, *Tetrahedron* **1968**, *24*, 1083.

[23] Experimental procedures as well as full spectroscopic and analytical data for compounds not included in this Experimental Section are described in the Supporting Information. It contains as well copies of NMR spectra for all new compounds.

[24] a) A. D. Becke, *J. Chem. Phys.* **1993**, *98*, 5648; b) C. Lee, W. Yang, R. G. Parr, *Phys. Rev. B* **1988**, *37*, 785.

[25] W. J. Hehre, L. Radom, P. v. R. Schleyer, J. A. Pople, *Ab initio Molecular Orbital Theory*, Wiley, New York, **1986**.

[26] a) E. Cances, B. Mennucci, J. Tomasi, *J. Chem. Phys.* **1997**, *107*, 3032; b) M. Cossi, V. Barone, R. Cammi, J. Tomasi, *Chem. Phys. Lett.* **1996**, *255*, 327; c) V. Barone, M. Cossi, J. Tomasi, *J. Comput. Chem.* **1998**, *19*, 404.

[27] a) H. B. Schlegel, *J. Comput. Chem.* **1982**, *3*, 214; b) H. B. Schlegel, *Geometry Optimization on Potential Energy Surface*, in: *Modern Electronic Structure Theory*, (Ed.: D. R. Yarkony), World Scientific Publishing, Singapore, **1994**.

[28] K. Fukui, *J. Phys. Chem.* **1970**, *74*, 4161.

[29] a) C. González, H. B. Schlegel, *J. Phys. Chem.* **1990**, *94*, 5523; b) C. González, H. B. Schlegel, *J. Chem. Phys.* **1991**, *95*, 5853.

[30] a) A. E. Reed, R. B. Weinstock, F. Weinhold, *J. Chem. Phys.* **1985**, *83*, 735; b) A. E. Reed, L. A. Curtiss, F. Weinhold, *Chem. Rev.* **1988**, *88*, 899.

[31] M. J. Frisch, G. W. Trucks, H. B. Schlegel, G. E. Scuseria, M. A. Robb, J. R. Cheeseman, J. A. Montgomery, T. Vreven, K. N. Kudin, J. C. Burant, J. M. Millam, S. S. Iyengar, J. Tomasi, V. Barone, B. Mennucci, M. Cossi, G. Scalmani, N. Rega, G. A. Petersson, H. Nakatsuji, M. Hada, M. Ehara, K. Toyota, R. Fukuda, J. Hasegawa, M. Ishida, T. Nakajima, Y. Honda, O. Kitao, H. Nakai, M. Klene, X. Li, J. E. Knox, H. P. Hratchian, J. B. Cross, C. Adamo, J. Jaramillo, R. Gomperts, R. E. Stratmann, O. Yazyev, A. J. Austin, R. Cammi, C. Pomelli, J. W. Ochterski, P. Y. Ayala, K. Morokuma, G. A. Voth, P. Salvador, J. J. Dannenberg, V. G. Zakrzewski, S. Dapprich, A. D. Daniels, M. C. Strain, O. Farkas, D. K. Malick, A. D. Rabuck, K. Raghavachari, J. B. Foresman, J. V. Ortiz, Q. Cui, A. G. Baboul, S. Clifford, J. Cioslowski, B. B. Stefanov, G. Liu, A. Liashenko, P. Piskorz, I. Komaromi, R. L. Martin, D. J. Fox, T. Keith, M. A. Al-Laham, C. Y. Peng, A. Nanayakkara, M. Challacombe, P. M. W. Gill, B. Johnson, W. Chen, M. W. Wong, C. Gonzalez, J. A. Pople, *Gaussian 03*, Gaussian, Inc., Wallingford CT, **2004**.

